

Stouffer

NRL Report 7888

Crack-Length Determination for the Compact Tension Specimen Using a Crack-Opening-Displacement Calibration

A. M. SULLIVAN

*Strength of Metals Branch
Engineering Materials Division*

June 24, 1975



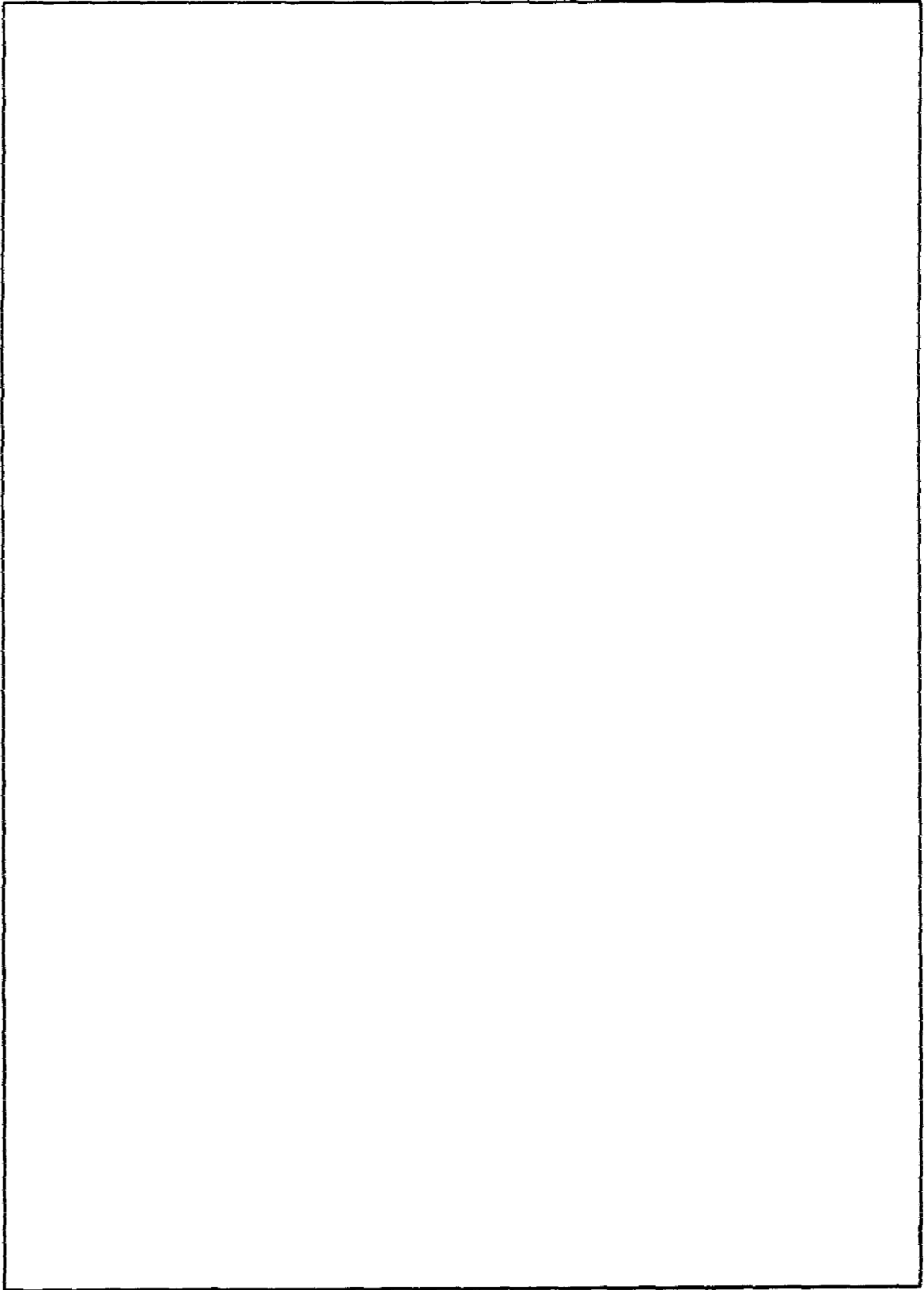
NAVAL RESEARCH LABORATORY
Washington, D.C.

Approved for public release; distribution unlimited.



REPORT DOCUMENTATION PAGE		READ INSTRUCTIONS BEFORE COMPLETING FORM
1. REPORT NUMBER NRL Report 7888	2. GOVT ACCESSION NO.	3. RECIPIENT'S CATALOG NUMBER
4. TITLE (and Subtitle) CRACK-LENGTH DETERMINATION FOR THE COMPACT TENSION SPECIMEN USING A CRACK- OPENING-DISPLACEMENT CALIBRATION		5. TYPE OF REPORT & PERIOD COVERED Final report on one phase of a continuing NRL problem.
		6. PERFORMING ORG. REPORT NUMBER
7. AUTHOR(s) A. M. Sullivan		8. CONTRACT OR GRANT NUMBER(s)
9. PERFORMING ORGANIZATION NAME AND ADDRESS Naval Research Laboratory Washington, D.C. 20375		10. PROGRAM ELEMENT, PROJECT, TASK AREA & WORK UNIT NUMBERS NRL Problem M01-24 Project RR 022-01-46-5431
11. CONTROLLING OFFICE NAME AND ADDRESS Department of the Navy Office of Naval Research Arlington, VA 22217		12. REPORT DATE June 24, 1975
		13. NUMBER OF PAGES 18
14. MONITORING AGENCY NAME & ADDRESS (If different from Controlling Office)		15. SECURITY CLASS. (of this report) Unclassified
		15a. DECLASSIFICATION/DOWNGRADING SCHEDULE
16. DISTRIBUTION STATEMENT (of this Report) Approved for public release; distribution unlimited.		
17. DISTRIBUTION STATEMENT (of the abstract entered in Block 20, if different from Report)		
18. SUPPLEMENTARY NOTES		
19. KEY WORDS (Continue on reverse side if necessary and identify by block number) Calibration Compliance Clip gage Crack-opening displacement (COD) Compact tension (CT) specimen Fatigue crack growth rate		
20. ABSTRACT (Continue on reverse side if necessary and identify by block number) A normalized calibration curve using clip-gage measurements of crack-opening-displacement (COD) at the crack mouth has been developed for the compact tension (CT) specimen. This procedure provides a simple, indirect determination of crack length during cyclic loading and is well adapted for automation of fatigue crack-growth-rate (FCGR) tests. The specific CT specimen configuration studied was the same as that employed in a recent interlaboratory FCGR testing program conducted by ASTM Sub-committee E24.04 on Subcritical Crack Growth.		

SECURITY CLASSIFICATION OF THIS PAGE(When Data Entered)



CONTENTS

SYMBOLS	iv
INTRODUCTION	1
EXPERIMENTAL CONSIDERATIONS	2
Material	2
Specimen Configuration	2
Test Procedure	2
Data Reduction	5
COD CALIBRATION CURVE	5
COMPARISON WITH CALCULATED COMPLIANCE VALUES	7
CONCLUSIONS	13
ACKNOWLEDGMENT	14
REFERENCES	14

SYMBOLS

a	Total crack length of the CT specimen measured from the load point
a/W	Crack length-to-width ratio; a zero subscript denotes an initial value
B	Specimen thickness
COD	Crack-opening displacement
CF	Correction factor
CT	Compact tension specimen
E	Young's modulus
FCGR	Fatigue crack growth rate
\dot{G}	Strain energy release rate
h	Half height of the CT specimen
K	Stress-intensity factor
ΔK	Stress-intensity factor range ($K_{\max} - K_{\min}$)
MAT	Material
P	Load
V	Half total displacement in the compliance measurement
W	Specimen width at load point
W_T	Specimen width at the measuring point

CRACK-LENGTH DETERMINATION FOR THE COMPACT TENSION SPECIMEN USING A CRACK-OPENING-DISPLACEMENT CALIBRATION

INTRODUCTION

Although at present no standards are available for fatigue crack-growth-rate (FCGR) testing, considerable research effort is being expended in this direction. In March of 1970 a special Task Group (E24.04.01 on Fatigue Crack Growth Rate Testing) was organized within Subcommittee 4 (Subcritical Crack Growth) of ASTM Committee E-24 on Fracture Testing of Metals to provide the basic information required for the development of a recommended procedure for FCGR testing. This ASTM Task Group has conducted a successful extensive interlaboratory (round robin) testing program to identify and characterize the sources of variability and bias inherent in FCGR testing. A Task Group report on this program has been published [1].

The ASTM round-robin program used optical surface measurements to determine crack length in two types of fracture mechanics specimens, center-cracked tension (CCT) and compact tension (CT). The ASTM Task Group report [1] identifies crack-length determination as a primary source of variability in FCGR testing. In addition to being error prone, due to operator bias and crack-front irregularity, visual determination of crack length is time consuming and incompatible with the trend towards automated testing.

An alternative method, measurement of the crack-opening displacement (COD) and determination of crack length from a normalized calibration curve of $EB[COD]/P$ vs a/W , has several distinct advantages over optical techniques. The COD measurements average out crack-front irregularities which may not be apparent from optical surface observations, include the plastic zone in estimations of crack length so that in the calculation of ΔK no correction for the plastic zone need be made, and readily provide an analog signal for instrumented testing.

Although this technique has been used reliably for determining crack growth in thin-sheet plane-stress K_{Ic} specimens [2], its application to crack growth under cyclic loading is neither widespread nor well documented. To insure confidence in its reliability, a program was inaugurated to develop a suitable calibration curve for the ASTM E24.04 CT specimen. This could then be used in a series of tests on different alloys to compare to the results of optically and COD-calibration-determined crack lengths and the subsequent da/dN vs ΔK log-log plots.

EXPERIMENTAL CONSIDERATIONS

Material

Alloys from three different metal systems—aluminum, titanium, and steel—were used for these tests. These are described in Table 1.

Table 1
Specimens Used for the Calibration

Material	Thickness (in.)	a/W						σ_{ys}^* (ksi)	K_{Ic}^* (ksi $\sqrt{\text{in.}}$)
		0.20	0.30	0.35	0.40	0.50	0.60		
7075-T6 aluminum	0.25		x	x	x			82	25
	0.50	x	x	x		x	x		
2024-T351 aluminum	0.25		x	x	x	x		49	31
	1.00		x	x	x	x	x		
Ti-6Al-4V	0.50		x	x	x	x		135	57
4340 steel	1.00		x	x	x	x		180	150

*Nominal value.

Specimen Configuration

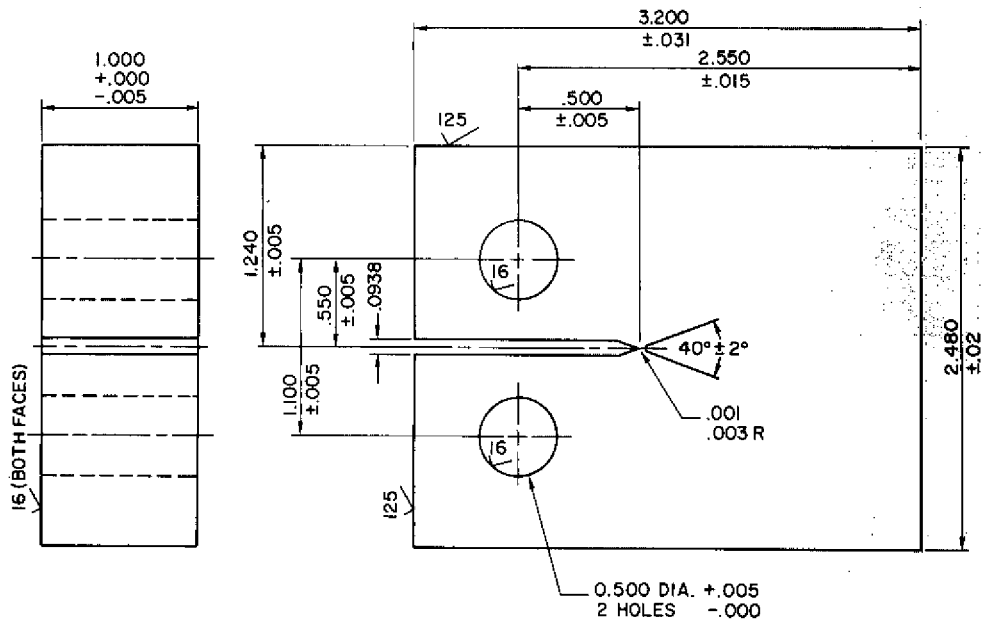
The CT specimen was used and is shown in Fig. 1. This specimen is not only economical of material but also of testing-machine loading capacity. The dimensions shown here were chosen to conform with those selected for the ASTM round-robin program [1] so that comparative data could be produced. Specimens were prepared with machined notches conforming to various a/W values, as outlined in Table 1.

Test Procedure

Each specimen was extended in tension to a load predetermined to be well below that required for K_{Ic} determination so that an elastic response could be insured.

The COD measurements were made using an MTS clip gage, the notched arms of which fit over knife edges screwed onto the specimen to straddle the mouth of the slit (Fig. 2). Knife-edge separation was 0.475 in. (11.8 mm) but measurement was over 1.1 in. (27.5 mm), the position of the first set of holding screws. Although a more recent model of this gage with a knife-edge separation of 0.2 in. (5.1 mm) and holding-screw separation of 0.8 in. (20.4 mm) is considered preferable, it is unlikely that this minor difference will affect the calibration.

Signals from the strain-gage circuit were fed into a Hewlett-Packard XY recorder together with those from the load cell of a 100-kip-capacity MTS closed-loop testing machine.



ASTM/NRL COMPACT TENSION CRACK GROWTH SPECIMEN

Fig. 1—Configuration of the compact tension specimen

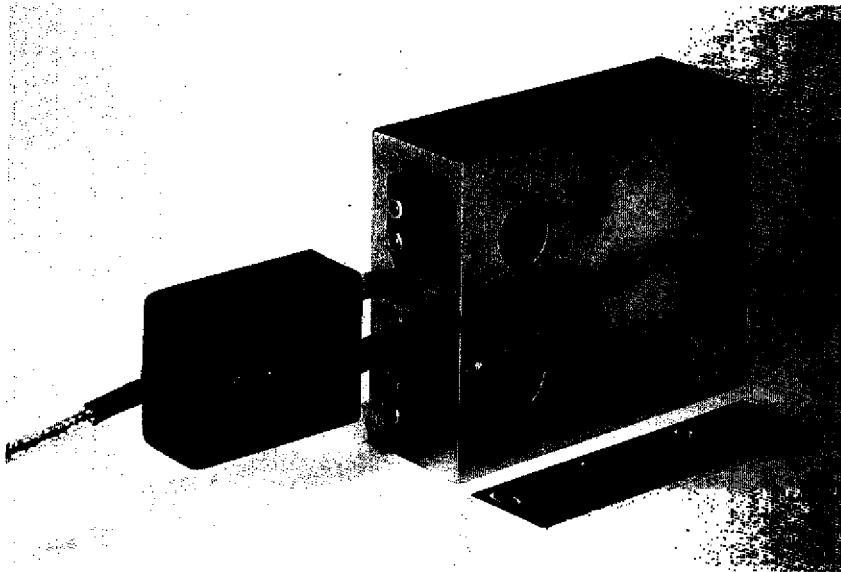
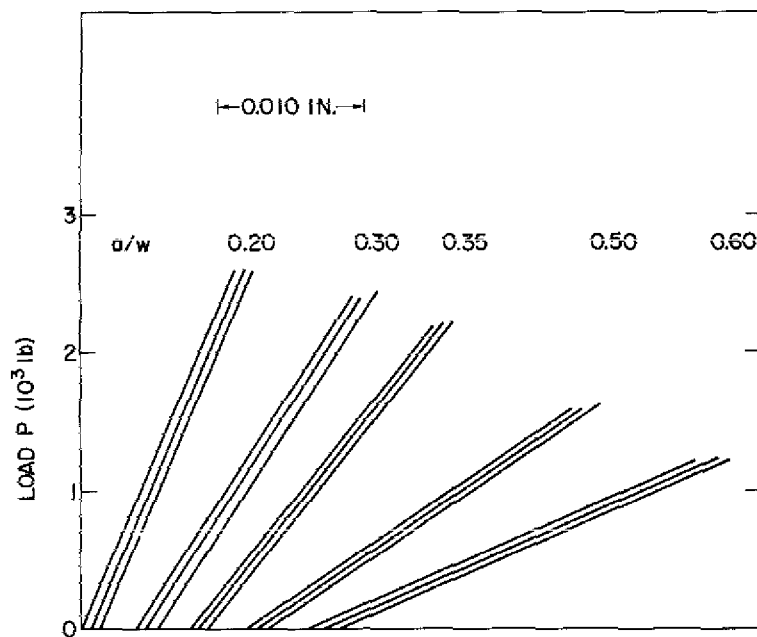
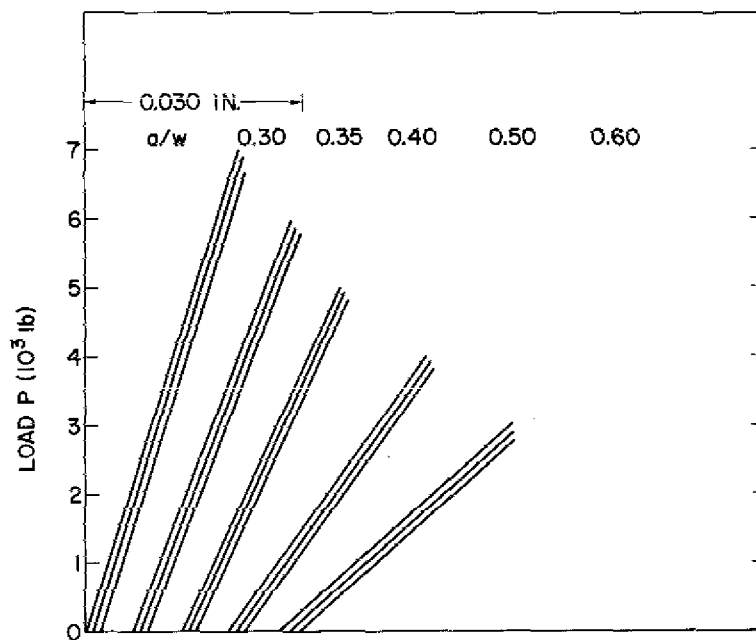


Fig. 2—Specimen with the clip gage attached

The specimens were positioned in the pin-loaded grips of the testing machine, three loadings and curve traces being made to the appropriate maximum load. The specimens were then removed and repositioned in the grips, and three more loadings were made. Figures 3a and 3b show typical traces of P vs COD.



(a) 7075-T6 aluminum, $B = 0.50$ in.



(b) 2024-T351 aluminum, $B = 1.00$ in.

Fig. 3—Experimental load-vs-displacement curves (P vs COD) for two series of calibrations

Data Reduction

Angles of the load-COD curves were read using a drafting machine. The angle cotangents, multiplied by appropriate 45°-angle units, modulus E , and thickness B , give values of $EB[\text{COD}]/P$. Since exact values of E were not known for all materials, data from aluminum alloy 7075-T6 were used as standard values, material E being calculated as

$$E_{\text{MAT}} = \left[\frac{EB[\text{COD}]}{P} \right]_{7075\text{-T6}} \left[\frac{P}{B[\text{COD}]} \right]_{\text{MAT}} \quad (1)$$

Values of E determined in this manner were used to normalize 2024-T351 aluminum, Ti-6Al-4V, and 4340 steel data. Values for each set of runs for each material are listed in Table 2. Average values for all four materials are listed in Table 3. Data appeared to be very reproducible.

COD CALIBRATION CURVE

A calibration curve of $EB[\text{COD}]/P$ vs a/W , using average values, is presented in Fig. 4. To determine unknown crack-length values, the reciprocal slope $P/[\text{COD}]$ is calculated from the P -vs-COD curve and normalized using values of thickness B and modulus E for the particular specimen under test. The value computed for the $(a/W)_0$ trace is compared with the calibration value, and adjustments are made in the values calculated after crack growth has occurred. Then a/W is read on the calibration curve for this value of $EB[\text{COD}]/P$, and a is calculated from the particular specimen width W , provided that the half-height-to-width ratio, h/W , remains constant. Crack-growth increments of 0.025 in. (0.6 mm) or more are reliably measured using this procedure.

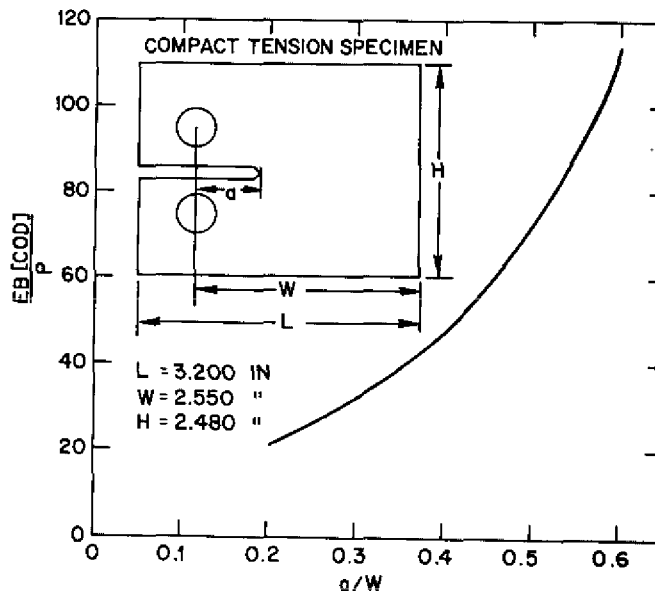


Fig. 4—Normalized calibration curve, $EB[\text{COD}]/P$ vs a/W

Table 2
Calibration EB[COD]/P Data* From All Tests

Material	Thickness (in.)	E × 10 ⁶ (p.s.i.)	a/W					
			0.20	0.30	0.35	0.40	0.50	0.60
7075-T6 aluminum	0.25 [†]	10.4	—	32.7	38.8	47.8	—	—
	0.25 [‡]	10.4	—	32.1	38.4	47.5	—	—
	Average:	10.4	—	32.4	38.6	47.6	—	—
	0.50 [†]	10.4	20.7	31.9	39.4	—	73.2	113.6
	0.50 [‡]	10.4	20.9	31.8	39.4	—	72.3	113.6
	Average:	10.4	20.8	31.8	39.4	—	72.7	113.6
	Grand Average:	10.4	20.8	32.1	39.0	47.6	72.7	113.6
2024-T351 aluminum	0.25 [†]	10.7	—	32.1	39.2	47.6	72.3	—
	0.25 [‡]	10.7	—	31.8	39.1	48.2	72.5	—
	Average:	10.7	—	32.0	39.2	47.9	72.4	—
	1.00 [†]	10.6	—	32.2	39.1	46.6	72.7	117.0
	1.00 [‡]	10.6	—	31.8	39.1	46.4	72.5	113.7
	Average:	10.6	—	32.0	39.1	46.5	72.6	113.8
	Grand Average:	10.7	—	32.0	39.1	46.6	72.6	113.8
Ti-6Al-4V	0.50 [†]	16.1	—	31.7	38.9	47.4	74.4	—
	0.50 [‡]	17.0	—	31.8	38.2	47.1	74.0	—
	Average:	16.6	—	31.8	38.6	47.2	74.2	—
4340 steel	1.00 [†]	30.4	—	32.2	39.5	48.6	72.0	—
	1.00 [‡]	29.9	—	32.0	39.2	48.1	72.4	—
	1.00 [§]	30.2	—	32.0	38.9	47.8	72.3	—
	Average:	30.2	—	32.1	39.2	48.2	72.2	—

*At each value of a/W, three traces (P vs COD) were made and values averaged to give EB[COD]/P.

[†]First set of calibration curves.

[‡]Second set of calibration curves.

[§]Third set of calibration curves.

Table 3
Grand Average Calibration of EB[COD]/P

Material	E × 10 ⁶ (p.s.i.)	a/W					
		0.20	0.30	0.35	0.40	0.50	0.60
7075-T6 aluminum	10.4	20.8	32.1	39.0	47.6	72.7	113.6
2024-T351 aluminum	10.7	—	32.0	39.1	46.6	72.6	113.8
Ti-6Al-4V	16.4	—	31.8	38.6	47.2	74.2	—
4340 steel	30.2	—	32.1	39.2	48.2	72.2	—
		20.8 avg.	32.0 avg.	39.0 avg.	47.4 avg.	72.9 avg.	113.7 avg.

To minimize operator bias and further advance the prospect of automation, a polynomial expression has been fitted to the data points to give

$$\frac{\text{EB}[\text{COD}]}{P} = -14.07 + 278.2 \frac{a}{W} - 726.0 \left(\frac{a}{W}\right)^2 + 1036.0 \left(\frac{a}{W}\right)^3 \quad (2)$$

or

$$\left(\frac{a}{W}\right) = -0.06209 + 0.01520 \left(\frac{\text{EB}[\text{COD}]}{P}\right) - 0.000141 \left(\frac{\text{EB}[\text{COD}]}{P}\right)^2 + 0.000000524 \left(\frac{\text{EB}[\text{COD}]}{P}\right)^3 \quad (3)$$

Values computed from these expressions compare favorably with those experimentally determined (Tables 4a and 4b). Further, values of a/W determined by Eq. (3) from the same set of P-vs-COD curves read by two operators and evaluated for EB[COD]/P were virtually identical, whereas estimates from the curve were somewhat discrepant.

COMPARISON WITH CALCULATED COMPLIANCE VALUES

The measurement of COD must not be confused with compliance measurement. Compliance is an energy measurement from which values of \mathcal{G} (and thereby K) can be

Table 4a
Comparison of Calibration and Calculated
Values of $EB[COD]/P$

a/W	Calibration	Calculated
0.2	20.8	20.8
0.3	32.0	32.0
0.4	47.4	47.4
0.5	72.9	73.0
0.6	113.7	115.2

Table 4b
Comparison of Calibration and Calculated
Values of a/W

$EB[COD]/P$	Calibration	Calculated
20	0.195	0.190
40	0.355	0.354
60	0.450	0.455
80	0.520	0.520
100	0.570	0.572

determined [3]. Manipulations of the equations involved can give the shape of the compliance curve relative to a/W as follows:

(a) K calculation for the CT specimen [4]:

$$K = \frac{P}{BW} a^{1/2} Y_a \quad (4)$$

when $h/W = 0.486$,

$$Y_a = 30.96 - 195.8 \frac{a}{W} + 730.6 \left(\frac{a}{W}\right)^2 - 1186.3 \left(\frac{a}{W}\right)^3 + 754.6 \left(\frac{a}{W}\right)^4, \quad (5)$$

where

B = specimen thickness

W = specimen width

h = half specimen height

a = crack length

and

P = load.

Some values of Y are listed in Table 5.

Table 5
Values of Correction Factor Y_a

a/W	Y_a	a/W	Y_a
0.20	12.74	0.40	12.93
0.30	12.06	0.50	14.58
0.35	12.39	0.60	18.05

(b) K compliance relationship:

$$K^2 = E\mathcal{G} = \frac{E}{2} \left(\frac{P}{BW} \right)^2 W^2 \frac{d \left(\frac{BW}{P} \frac{2V}{W} \right)}{da}, \quad (6)$$

where

E = Young's Modulus

and

$2V$ = total displacement.

To equate these expressions, Eq. (4) becomes

$$K = \frac{P}{BW} W^{1/2} Y_b, \quad (7)$$

where

$$Y_b = 29.6 \left(\frac{a}{W} \right)^{1/2} - 185.8 \left(\frac{a}{W} \right)^{3/2} + 655.7 \left(\frac{a}{W} \right)^{5/2} - 1017.0 \left(\frac{a}{W} \right)^{7/2} + 638.9 \left(\frac{a}{W} \right)^{9/2}. \quad (8)$$

Equation (6) becomes

$$K^2 = E\mathcal{G} = \frac{E}{2} \left(\frac{P}{BW} \right)^2 W \frac{d \left(\frac{BW}{P} \frac{2V}{W} \right)}{d \left(\frac{a}{W} \right)}. \quad (9)$$

Then

$$K^2 = \left(\frac{P}{BW}\right)^2 W Y_b^2 = \frac{E}{2} \left(\frac{P}{BW}\right)^2 W \frac{d \left(\frac{BW}{P} \frac{2V}{W}\right)}{d \left(\frac{a}{W}\right)}, \quad (10)$$

so that finally

$$E \frac{d \left(\frac{BW}{P} \frac{2V}{W}\right)}{d \left(\frac{a}{W}\right)} = 2Y_b^2 \quad (11)$$

and

$$\begin{aligned} (Y_b)^2 = & 958.52 \frac{a}{W} - 12,123.94 \left(\frac{a}{W}\right)^2 + 83,576.40 \left(\frac{a}{W}\right)^3 \\ & - 359,558.66 \left(\frac{a}{W}\right)^4 + 1,045,056.27 \left(\frac{a}{W}\right)^5 \\ & - 2,028,922.92 \left(\frac{a}{W}\right)^6 + 2,509,929.21 \left(\frac{a}{W}\right)^7 \\ & - 1,790,363.96 \left(\frac{a}{W}\right)^8 + 569,421.16 \left(\frac{a}{W}\right)^9. \end{aligned} \quad (12)$$

Integrating:

$$\frac{EB[2V]}{P} = 2 \int Y_b^2 d\left(\frac{a}{W}\right), \quad (13)$$

and

$$\begin{aligned} \frac{EB[2V]}{P} = & 479.26 \left(\frac{a}{W}\right)^2 - 4,041.31 \left(\frac{a}{W}\right)^3 + 20,894.10 \left(\frac{a}{W}\right)^4 \\ & - 71,911.73 \left(\frac{a}{W}\right)^5 + 174,176.04 \left(\frac{a}{W}\right)^6 \\ & - 289,846.13 \left(\frac{a}{W}\right)^7 + 313,741.15 \left(\frac{a}{W}\right)^8 \\ & - 198,929.32 \left(\frac{a}{W}\right)^9 + 56,942.12 \left(\frac{a}{W}\right)^{10} + C, \end{aligned} \quad (14)$$

where C is the constant of integration and can be neglected since slopes only are used in the calculations.

The values of $EB[2V]/P$ determined in this manner are those at the loading point, that is, directly under the pins. However, the measurement of COD is at the crack mouth, which is at a fixed distance from the load point; therefore, values of $2V$ are computed for this position by triangulation:

$$\left[\frac{EB[2V]}{P} \right]_{\text{measuring point}} = \left[\frac{EB[2V]}{P} \right]_{\text{load point}} \cdot \frac{a + (W_T - W)}{a} \quad (15)$$

Values of this correction factor CF are provided in Table 6, and comparative values are contained in Table 7.

Table 6
Correction Factor CF From the Load Point to the Measuring Point

$$W = 2.55; \quad W_T = 3.20; \quad h/W = 0.486;$$

$$CF = [a + (W_T - W)]/a = (a + 0.650)/a$$

a/W	a	$a + 0.6500$	CF
0.20	0.5100	1.1600	2.2745
0.30	0.7650	1.4150	1.8500
0.35	0.8925	1.5925	1.7283
0.40	1.0200	1.6700	1.6372
0.50	1.2750	1.9250	1.5098
0.60	1.5300	2.1800	1.4248

Table 7
Comparative Values of $EB[COD]/P$ and
 $EB[2V]/P$; $h/W = 0.486$

a/W	$\frac{EB[COD]}{P}$, Calibration Value	$\frac{EB[2V]}{P}$, Calculated at the Measuring Point	$\frac{EB[2V]}{P}$, Calculated at the Load Point
0.20	20.8	24.6	10.8
0.30	32.0	33.6	18.2
0.35	39.0	39.6	22.9
0.40	47.4	47.5	29.0
0.50	72.9	69.4	46.0
0.60	113.7	100.5	70.6

Table 8 contains values of the derivative computed from Eqs. (13), (14), and (15) and compared with those determined graphically from Figs. 4 and 5.

Table 8
Comparative Values of the Derivatives; $h/W = 0.486$

a/W	$\frac{d(EB[2V]/P)}{d(a/W)}$ Computed	$\frac{d(EB[2V]/P)}{d(a/W)}$ From the Curve at the Load Point	$\frac{d(EB[2V]/P)}{d(a/W)}$ From the Curve at the Measuring Point	$\frac{d(EB[COD]/P)}{d(a/W)}$ From the Curve of the Calibration Values
0.20	64.8	42.4	53.6	72.8
0.30	87.2	89.1	117.8	129.8
0.35	107.4	110.8	134.9	164.8
0.40	133.7	134.4	181.3	189.8
0.50	212.5	200.0	247.0	285.6
0.60	391.0	346.4	320.1	401.1

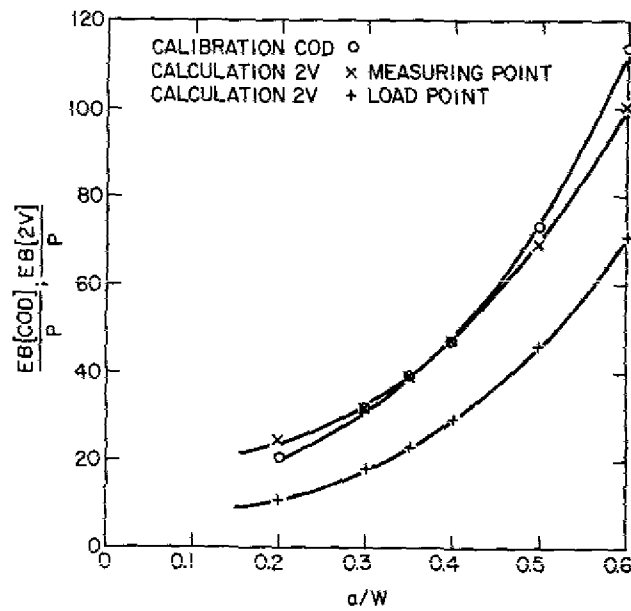


Fig. 5—Comparison of the normalized calibration curve with the computed compliance curve

From Eq. (5):

$$\frac{K}{\frac{P}{BW} W^{1/2}} = Y_b \quad (16)$$

$$Y_b = \left(\frac{a}{W}\right)^{1/2} Y_a \quad (17)$$

From Eq. (6):

$$\frac{K}{\frac{P}{BW} W^{1/2}} = \sqrt{\frac{E}{2} \frac{d\left(\frac{BW}{P} \frac{2V}{W}\right)}{d\left(\frac{a}{W}\right)}} \quad (18)$$

These normalized values are compared in Table 9. Calculation from Eq. (18) is redundant but serves to check the arithmetic which is cumbersome.

Table 9
Comparative Values of $K(P/BW)^{-1} W^{-1/2} = \sqrt{1/2[d(EB[2V]/P)/d(aW)]}$; $h/W = 0.486$

a/W	From Y_a and Eqs. (1), (2), (3), and (14)	From the Computed Derivative	From the Measured Slope at the Load Point	From the Measured Slope at the Measuring Point	From the Measured Slope of the Calibration Curve
0.20	5.7	5.7	4.6	5.2	6.0
0.30	6.6	6.6	6.6	7.6	8.1
0.35	7.3	7.3	7.4	8.2	9.1
0.40	8.2	8.2	8.2	9.5	9.7
0.50	10.2	10.3	10.0	11.1	11.9
0.60	14.0	14.0	13.2	12.6	14.2

CONCLUSIONS

- Normalized calibration curves of $EB[COD]/P$ vs a/W determined from CT specimens of varied thickness representing three alloy systems compare accurately with one another.

- Therefore a "master curve" from these calibrations can be used to determine crack length with the ASTM E24.04 CT specimen.

- This COD calibration curve is not to be confused with the compliance curve, the derivative of which can be used for the computation of fracture resistance K values.

ACKNOWLEDGMENT

The technical assistance provided by G. W. Jackson enabled the accurate and rapid development of this calibration. The financial support of the Office of Naval Research is gratefully acknowledged.

REFERENCES

1. W.G. Clark, Jr., and S.J. Hudak, Jr., "Variability in Fatigue Crack Growth Rate Testing—An ASTM E24.04.01 Task Group Report," Westinghouse Research Laboratories, Pittsburgh, PA, Scientific Paper 74-1E7-MSLRA-P2 (1974).
2. A.M. Sullivan and C.N. Freed, "A Review of the Plane-Stress Fracture Mechanics Parameter K_c Determined Using the Center-Cracked Tension Specimen," NRL Report 7460, Dec. 29, 1972.
3. G.R. Irwin, "Fracture Testing of High-Strength Sheet Materials Under Conditions Appropriate for Stress Analysis," NRL Report 5486, July 27, 1960.
4. E.T. Wessel, "State of the Art of the WOL Specimen for K_{Ic} Fracture Toughness Testing," *Engineering Fracture Mechanics* 1, 77 (1968).

From Eq. (5):

$$\frac{K}{\frac{P}{BW} W^{1/2}} = Y_b \quad (16)$$

$$Y_b = \left(\frac{a}{W}\right)^{1/2} Y_a \quad (17)$$

From Eq. (6):

$$\frac{K}{\frac{P}{BW} W^{1/2}} = \sqrt{\frac{E}{2} \frac{d\left(\frac{BW}{P} \frac{2V}{W}\right)}{d\left(\frac{a}{W}\right)}} \quad (18)$$

These normalized values are compared in Table 9. Calculation from Eq. (18) is redundant but serves to check the arithmetic which is cumbersome.

Table 9
Comparative Values of $K(P/BW)^{-1} W^{-1/2} = \sqrt{1/2[d(EB[2V]/P)/d(aW)]}$; $h/W = 0.486$

a/W	From Y_a and Eqs. (1), (2), (3), and (14)	From the Computed Derivative	From the Measured Slope at the Load Point	From the Measured Slope at the Measuring Point	From the Measured Slope of the Calibration Curve
0.20	5.7	5.7	4.6	5.2	6.0
0.30	6.6	6.6	6.6	7.6	8.1
0.35	7.3	7.3	7.4	8.2	9.1
0.40	8.2	8.2	8.2	9.5	9.7
0.50	10.2	10.3	10.0	11.1	11.9
0.60	14.0	14.0	13.2	12.6	14.2

CONCLUSIONS

- Normalized calibration curves of $EB[COD]/P$ vs a/W determined from CT specimens of varied thickness representing three alloy systems compare accurately with one another.
- Therefore a "master curve" from these calibrations can be used to determine crack length with the ASTM E24.04 CT specimen.
- This COD calibration curve is not to be confused with the compliance curve, the derivative of which can be used for the computation of fracture resistance K values.

ACKNOWLEDGMENT

The technical assistance provided by G. W. Jackson enabled the accurate and rapid development of this calibration. The financial support of the Office of Naval Research is gratefully acknowledged.

REFERENCES

1. W.G. Clark, Jr., and S.J. Hudak, Jr., "Variability in Fatigue Crack Growth Rate Testing—An ASTM E24.04.01 Task Group Report," Westinghouse Research Laboratories, Pittsburgh, PA, Scientific Paper 74-1E7-MSLRA-P2 (1974).
2. A.M. Sullivan and C.N. Freed, "A Review of the Plane-Stress Fracture Mechanics Parameter K_c Determined Using the Center-Cracked Tension Specimen," NRL Report 7460, Dec. 29, 1972.
3. G.R. Irwin, "Fracture Testing of High-Strength Sheet Materials Under Conditions Appropriate for Stress Analysis," NRL Report 5486, July 27, 1960.
4. E.T. Wessel, "State of the Art of the WOL Specimen for K_{Ic} Fracture Toughness Testing," *Engineering Fracture Mechanics* 1, 77 (1968).